SWISSMETRO
Polarized Linear Motor Combined With Levitation Actuators

A. Cassat*, C. Espanet**, V. Bourquin***, P. Hagmann****, M. Jufer*****

*, ***** *Ecole Polytechnique Fédérale de Lausanne, EPFL-STI-IPR-LAI, CH-1015, Lausanne, SWITZERLAND*
A. Cassat: Phone +41 21 693 2691, Facsimile +41 21 693 2687 M. Jufer: Phone +41 21 693 2684
** *University of Franche-Comté, France, Laboratory of Research in Electrical Engineering and Systems, L2ES/UTBM, rue Enest Thierry-Mieg, F-90010-Belfort cedex, FRANCE Phone +33 3 84 58 36 14, Facsimile +33 3 84 58 36 36*
*** *Numexia, PSE-A, CH-1015 Lausanne, SWITZERLAND Phone +41 21 693 8737*
**** *Ecole Polytechnique Fédérale de Lausanne, EPFL-STI-ISE-LIN - PSE-A, CH-1015 Lausanne, SWITZERLAND Phone +41 21 693 8737*

alain.cassat@epfl.ch, christophe.espanet@univ-fcomte.fr, vincent.bourquin@numexia.com, pascal.hagmann@epfl.ch, marcel.jufer@epfl.ch

Abstract SWISSMETRO is a MAGLEV Project, designed for a speed up to 500 km/h in two tunnels under partial vacuum. The authors investigate new possibilities to combine the propulsion and levitation. Polarized inductors for the levitation are studied, implying a polarized (permanent magnet) synchronous linear motor. The thermal behavior is investigated using a numerical platform of the complete vehicle-tunnel system and computational fluid dynamic analysis.

Keywords: Aerodynamic, Levitation, Linear motors, MAGLEV, permanent magnet, Swissmetro

1. SWISSMETRO – NEW VARIANTS

Swissmetro is a MAGLEV Project [1, 2], designed for speeds up to 500 km/h in two tunnels under partial vacuum, 8000 Pa. Initially, two propulsion variants (A, B, Table 5) are considered: A) the short stators of the linear homo-polar motors are fixed to the tunnel tracks; B) the stators of the motors are on board of the vehicles. The levitation, the guidance and the transfer of energy are independent functions. Variants A and B have technical issues to resolve, such as:

- a double motor inductor compensates the attractive force;
- the levitation and guidance inductors, not being polarized, the heat dissipation becomes an issue in partial vacuum, requiring a cooling system on board of the vehicle;
- a laminated reactive rail decreases the magnetic drag forces.

For a long stator fixed with the tunnel, the authors develop *new combinations of functions* [3] such as (Variants C, D, Table 5):

- the propulsion combined with the levitation, by attraction, uses permanent magnets for the excitation.

This paper presents the design key points of Variant D.

2. METHODS OF COMPUTATION

The motor design is based on three different methods:

- a lumped magnetic scheme [4] for a first order design;
- FEM [5] simulations confirm the chosen configurations. To simplify the FEM analysis, an equivalent 2D cylindrical and periodical system is defined End effects are neglected;
- The 3D numerical platform of HISTAR project [6] is used to compute the aerodynamics of the inductor mounted on the vehicle and the air flow and finally the heat transfer.

3. COMBINED PROPULSION WITH LEVITATION

3.1 DESCRIPTION The long stator, fixed with the tunnel, is a classical linear motor (Fig.1). The magnetic way, onboard of the vehicle, supports the excitation created by the permanent magnets and the inductor windings for the levitation control. An air gap of 20 mm is specified for the propulsion, the levitation and the guidance. Classical synchronous linear motors imply a short pole pitch of 231 mm. The maximum synchronous frequency is 300 Hz, corresponding to a speed of 500 km/h.

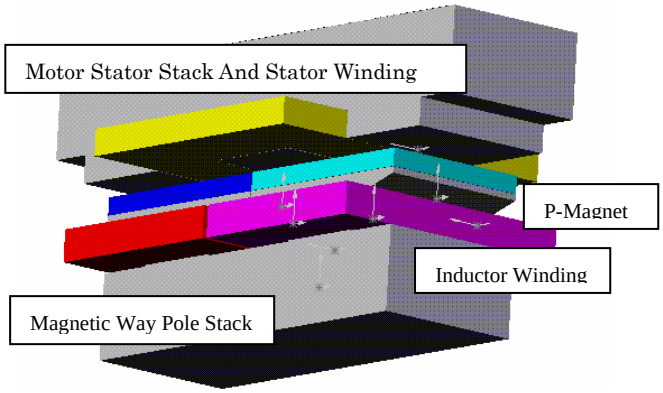

Fig. 1 Variant C, D: Combined propulsion with levitation

3.2 WINDING CONFIGURATION The winding (Variants C, D, Table 1) has a fractional number (q) of slots (Zn) per pole (2p) and per phase (m) and a coil opening (s) of one slot. The winding (Figure 2) has a copper filling factor greater than 0.5. The fundamental winding factor (kw1) is greater than 0.9. Full winding corresponds to one coil per slot; while half winding indicates two coils per slot, as shown in Figure 2.

Table 1. Winding configuration

Winding	Zn0	Zn	p	m	q	s	kw1
Variants A, B	57	54	7	3	1.86	3	0.9
Variants C, D	25	24	11	3	0.364	1	0.95

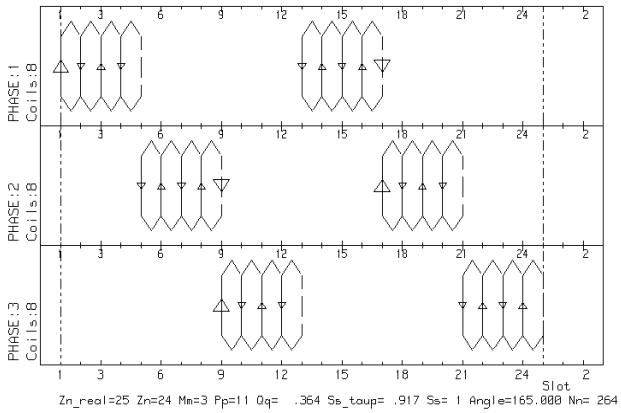

Fig. 2 Winding configuration: Variants C, D: half winding (two coils per slot)

3.3 MECHANICAL POWER The total mechanical power is 6 MW, see Specifications, Table 5. The magnetic ways are distributed in the four vehicle cells, the nose and the trail and on both vehicle sides. Consequently, each active part of the motors sees a twelveth of the total force and of the mechanical power. The motors produce a constant force until they reach their maximum mechanical power, than the acceleration is decreasing.

3.4 PERMANENT MAGNET The corresponding permanent magnet MMF is 13.1 kA, for a thickness of 16 mm NdFeB magnet and has a remanent flux density of 1.23 T.

3.5 MAGNETIC WAY IRON LOSSES The pole pitch of 231 mm and the active width of 90 mm require a decrease of the magnetic way iron losses. Laminations are necessary for the way yoke. For the PM pole, the thickness of the flux penetration is 31 mm. Consequently, the permanent magnet of one pole is segmented in the pole pitch direction (two cases: 4 and 8 segments) and in two segments in the active width direction. Table 2 shows the PM iron losses versus the stator tooth shape and the PM segmentation. Table 2 indicates that the stator tooth slot opening must be reduced (tooth shoe) and the PM segmented into eight parts, to limit the PM iron losses. Figure 3 shows the distribution of the flux for the two considered stator tooth shapes and for the two cases of PM segmentation (4 or 8 segments per pole). Figure 3 represents the flux distribution. Figure 4 shows the eddy current density in the PM segments for the chosen tooth shape and for the different segmentation cases. Figure 5 presents the air-gap flux density for the two cases of PM segmentation. For 8 segments, the distorsion of flux desity in motor mode is lower than in the case of 4 segments, explaining why the increase of the PM iron losses is lower in this case (128 kW instead of 343 kW). For the same stator MMF, Figure 6 shows the propulsion force, with and without segmented permanent magnets. The reduction of PM losses leads to an increase of the propulsion force.

Table 2. Permanent magnet iron losses, complete vehicle, speed 139 m/s

PM iron losses [kW] No load operation	PM iron losses [kW] Rated load operation	Tooth shoe	Segmented PM
2477	2712 (full winding)	no	no
67.7	374 (full winding)	yes	no
56.9	343 (full winding)	yes	yes (4)
28.5	128 (half winding)	yes	yes (8)

3.6 POWER BALANCE For a long stator, the stator duty cycle is defined in Equation (1). The frequency of vehicles per direction is each 6 min and the speed is v=139 m/s, for a stator section length of 5000 m, the duty cycle D is equal to 0.01.

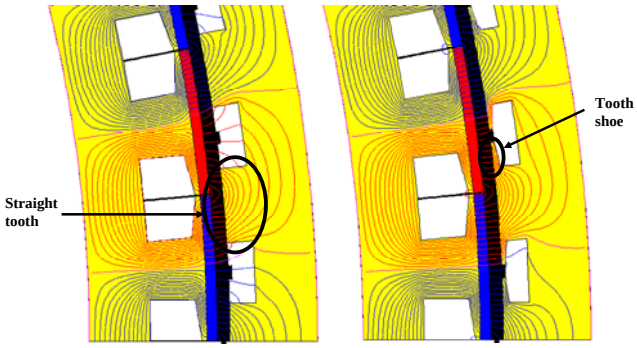

Fig. 3 Geometry and flux lines with stator straight tooth and with tooth shoe (no-load generator mode)

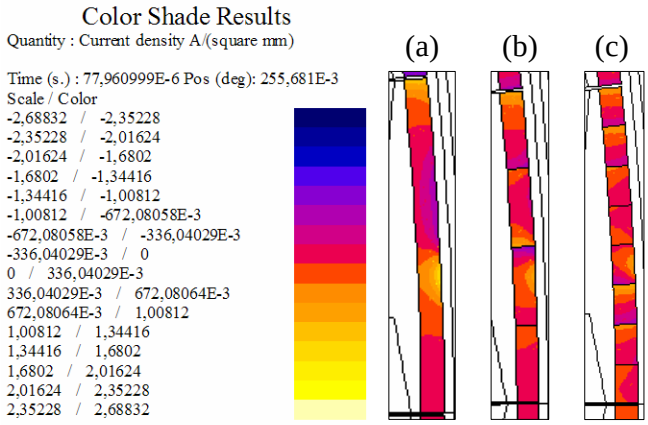

Fig. 4 PM eddy current density color shade (rated-load motor working)
(a) non segmented permanent magnets; (b) 4 segmentations; (c) 8 segmentions

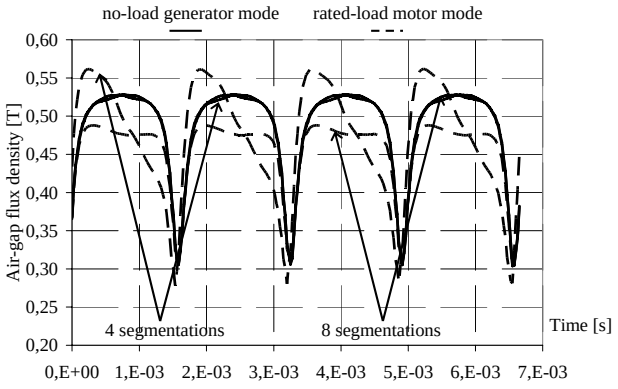

Fig. 5 Air-gap flux density (permanent magnets with 8 segments)

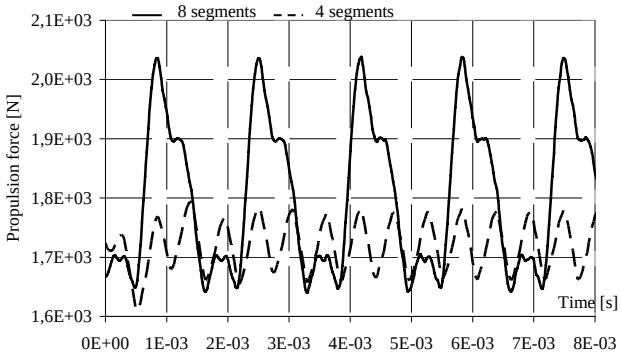

Fig. 6 Propulsion force (22 poles, permanent magnets with 8 segments)

The duty cycle of one stator sector is very low, consequently the heat dissipation at the level of the stator is not an issue. The stator current density can be increased to reduce the stator volume (reduction of the motor active width), then the stator Joule losses will increaase. On the other hand, there is a clear interest to fully use the complete length of the vehicle for the magnetic way, this will also reduce the motor active width. The efficiency is affected by the length of the stator section, which sees one motor inverter. The losses of the stator section part, which does not see an active part of the magnetic way, are the key components of the total losses. The efficiency can be determined from Equation (2):

$$D = \frac{l_{stator\ section\ length}}{v} \cdot \frac{1}{t_{frequency}} \quad (1)$$

$$\eta = \frac{Pmech}{Pmec + Piron_{total} + \frac{Pjoule}{l_{active}} \cdot l_{stator\ section\ length}} \quad (2)$$

Table 3 Total power balance corresponding to one vehicle

Mech	Stator		Magnetic way	
	Joule	Iron losses	Yoke	P-magnet
6 [MW]	17.4 [kW]	46.2 [kW]	11.6 [kW]	128 [kW]

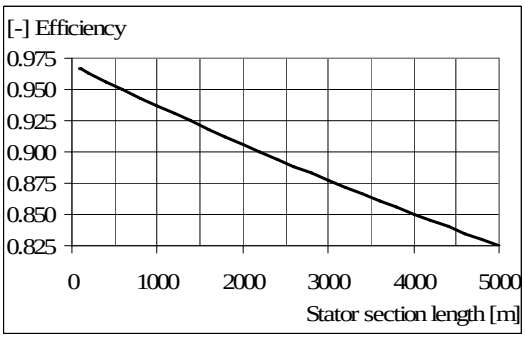

Fig. 7 Efficiency versus the stator section length

Table 3 shows the power balance for one vehicle. Figure 6 presents the efficiency as a function of the length of the stator section, indicating that an optimum must be defined between the stator investment costs, directly related to the current density and to the operational costs, related to consumption of energy. Furthermore, the energy consumption and the number of requested inverters depend on the stator section length. A complete economical optimization is therefore necessary.

3.7 CONVERTERS Each motor inverter is a three level input DC bus of 5, 0, -5 kV and a three phase inverter with three voltage levels, with GTO thyristors of 4500 V, 4000 A.

4. LEVITATION

4.1 DESIGN The additional inductor winding produces the necessary force complement (positive or negative) and assures the dynamic behavior of the inductor. The attractive force due to the permanent magnets, alone, should not result in a force higher than the vehicle weight with no passenger, but be a proportion of this weight. On the other hand, the mass of the vehicle varies between the mass without and with passengers, corresponding to a factor of 1.33. One pole produces an attractive force of 1.486 kN. The complete vehicle has 528 poles. Design and control strategies are given in Reference [3].

4.2 SIMULATIONS Figure 8 gives the evolution of the attraction force versus time and the vector forces are plotted around one stator tooth. It clearly shows two points. Firstly, the attraction force decreases in front of pole transition due to flux leakage between two consecutive poles. Secondly, the slot effect creates high attractive force ripples that may lead to vibration issues. Figure 9 shows the evolution of the attractive force versus the compensation MMF. The observed linear evolution means that the prevailing term is the one of interaction between the PM MMF and the compensation MMF inductor.

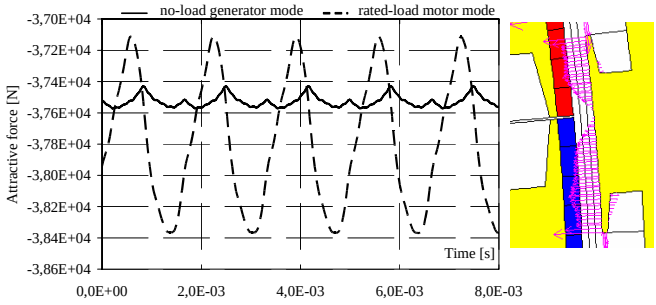

Fig. 8 Attraction force (22 poles with 8 segmentations of the PMs)

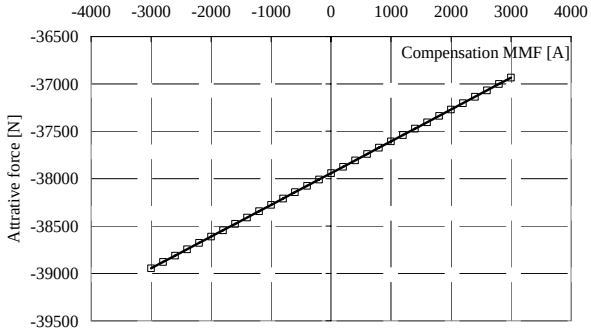

Fig. 9 Attraction force versus compensation MMF

4.3 THERMAL BEHAVIOR The pressure in the tunnel is reduced and thus, the capability of the flow to transfer heat through convection is questioned. 3D flow computations, using the commercial code FLUENT [7] enable an investigation of the spatial distribution of the pressure, the air flow speed and the temperature. Two approaches are investigated: Variants A, B - power dissipated on the wet area of the inductor itself (see Fig. 10) and Variants C, D - power dissipated distributed on the whole secondary structure on which the inductors are mounted (see Fig. 11). Figures 12 shows that, with the hypothesis of the whole heat losses concentrated on the inductor, excessively high temperatures are recorded. The flow around the bluff body of the inductor does not provide enough cooling without an additional system. In Figure 13, Variant D, the distribution of the power dissipated by electromechanical equipment on the whole secondary structure provides better cooling. This analysis shows that a lineic distribution (Variants C, D) of the heat losses and the use of as much of the secondary structure surface as a radiator is a solution for the heating problem in a partial vacuum environment.

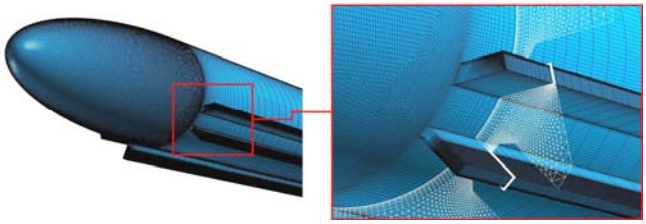

Fig. 10 Top right: one inductor located under the upper secondary structure.

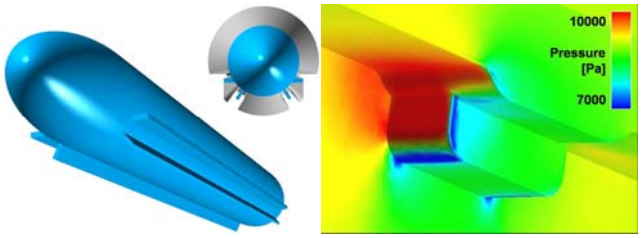

Fig. 11 Variants A, B: Geometry and pressure distribution, of one inductor

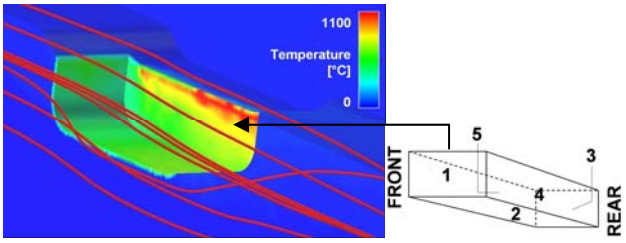

Fig. 12 Variants A, B Temperature distribution, of one inductor and urface definition

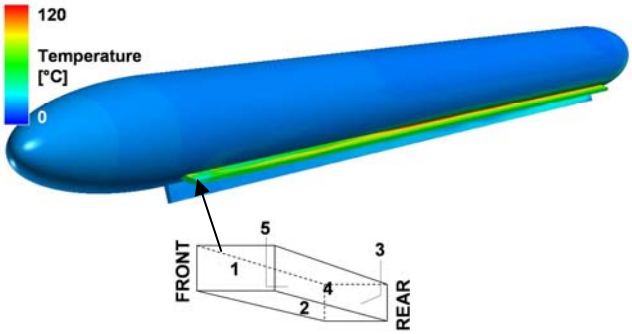

Fig. 13 Variant D: Temperature spatial distribution and surface definition

Table 4 Variants A, B, D: Temperatures and convection coefficients

Surface	Power	Wet area	T ambiant	T ave	T min	T max	Convection coefficient
	[W/m^2]	[m^2]	[°C]	[°C]	[°C]	[°C]	[W/ m^{2}K]
A, B, 1	30830	0.010	5.85	442	327	587	70.7
A, B, 2	30830	0.053	5.85	593	427	727	52.5
A, B, 3	30830	0.010	5.85	1098	577	1527	28.2
A, B, 4	30830	0.035	5.85	730	277	1407	42.6
A, B, 5	30830	0.035	5.85	872	327	1407	35.6
D, 1	996	0.073	5.85	48	27	67	23.4
D, 2	996	8.000	5.85	56	27	77	19.9
D, 3	996	0.073	5.85	74	52	112	14.5
D, 4	996	20.300	5.85	50	27	57	22.8
D, 5	996	25.760	5.85	80	27	137	13.5

Table 4 gives the temperatures and the convection coefficients on the surfaces described in Fig. 14, for the Variants A, B and D.

5. CONCLUSIONS

This paper is *a first order analysis* of the possible combination of the propulsion with the levitation. The concept optimization requires a more detailed technical investigation including a study of the energy and economy balances. The following points can be considered.

- The permanent magnet iron losses are a design constraints.
- The long stator and the choice of a classical stator winding, requires a deep investigation of the best possible winding configuration in order to decrease the PM losses.
- In a partial vacuum, the wetted area on which heat transfer occurs must be increased. The optimisation of the system from an energetic viewpoint is governed by a compromise between aerodynamic drag and heat transfer.

6. SPECIFICATIONS

Table 5 Specifications

Swissmetro Variants			**A**	**B**	**C**	**D**
	Acceleration	[m/s^2]	1.3	1.3	1.3	1.3
	Speed	[m/s]	139	139	139	139
	Frequency per direction	[sec]	360	360	360	360
Vehicle	Total mass	[ton]	80	80	80	80
	Total length	[m]	80	80	80	80
	Nb. of cells	[-]	4	4	4	4
	Nose length	[m]	15	15	15	15
	Tail length	[m]	15	15	15	15
	Cell length	[m]	12.5	12.5	12.5	12.5
	Nb. of passengers	[-]	200	200	200	200
	Propulsion in nose and tail		no	no	no	yes
Propulsion	Air gap	[m]	0.02	0.02	0.02	0.02
	Total mechanical power	[MW]	6	6	6	6
	Mech. power per section	[MW]	6	0.75	0.75	0.25
	Nb. of motors per cell	[-]	-	2	2	4
	Max. total propulsion force	[kN]	104	104	104	104
	Design speed	[m/s]	57.7	57.7	57.7	57.7
	Nb. of sections per cell	[-]	2	2	2	2
	Rotor section length	[m]	9.3	5.082	5.082	10.16
	Pole pitch	[m]	0.324	0.231	0.231	0.231
	Nb. of poles per section	[-]	-	22	22	44
Levitation	Air gap	[m]	0.02	0.02	0.02	0.02
	Nb. of poles per section	[-]	-	22	22	44
	Nb. of inductors per cell	[-]	4	44	44	88
	Force per inductor (pole)	[kN]	33	2.97	2.97	1.49
	Power loss (mean value)	[kW]	3.3	0.4	0.4	
	Mass of one inductor (pole)	[kg]	171	56	56	17

Variant A: short stators fixed with the tunnel

Variant B: stators on board of the vehicle

Variants C, D: long stator fixed with the tunnel, combined with levitation

References

(1) A. Cassat, "Electromécanique", SWISSMETRO - Main Study - Level B, Swissmetro SA, CP 5278, CH-1211 Genève, May 31, 1999.

(2) A. Cassat, V. Bourquin, M. Mossi, M. Badoux, D. Vernez, M. Jufer, N. Macabrey, P. Rossel, "SWISSMETRO - Project Development Status", International Symposium on Speed-up and Service Technology for Railway and Maglev Systems 2003 (STECH'03). 2003.8.19-22 Tokyo, Japan.

(3) A. Cassat, C. Espanet, "SWISSMETRO: Combined Propulsion with Levitation and Guidance", MAGLEV 2004, The 18th International Conference on Magnetically Levitated Systems and Linear Drives, October 26-28, 2004, Shanghai, China, Proceedings, pages: 747-758, vol. II.

(4) J. P. Wang, D. K. Lieu, W. L. Lorimer, A. Hartman "Comparison of Lumped Parameter and Finite Element Magnetic Modeling in Brushless DC Motor", IEEE Transactions on Magnetics, Vol. 33, No. 5, September 1997.

(5) FLUX2D/FLUX3D: Finite Element Software, Cedrat, Grenoble, France.

(6) M. Jufer, V. Bourquin, "Développement du projet Swissmetro par une plate-forme numérique", REE Revue de l'Electricité et de l'Electronique-SEE, Paris, No3, mars 2005, pp 97-101.

(7) FLUENT: 3D general-purpose CFD solver, Fluent France, Saint-Quentin en Yvelines, France